Earth and Planetary Science Letters 353–354 (2012) 231–239

Contents lists available at SciVerse ScienceDirect

# Earth and Planetary Science Letters

journal homepage: www.elsevier.com/locate/epsl

# Thermal and tectonic consequences of India underthrusting Tibet

Timothy J. Craig *, Alex Copley, James Jackson

*COMET+, Bullard Laboratories, Department of Earth Sciences, University of Cambridge, Cambridge CB3 0EZ, UK*

ARTICLE INFO

*Article history:*
Received 12 March 2012
Received in revised form
6 July 2012
Accepted 7 July 2012
Editor: P. Shearer

*Keywords:*
deep earthquakes
continental rheology
Tibet
temperature
Central Asian tectonics

ABSTRACT

The Tibetan Plateau is the largest orogenic system on Earth, and has been influential in our understanding of how the continental lithosphere deforms. Beneath the plateau are some of the deepest ( ~100 km) earthquakes observed within the continental lithosphere, which have been pivotal in ongoing debates about the rheology and behaviour of the continents. We present new observations of earthquake depths from the region, and use thermal models to suggest that all of them occur in material at temperatures of $\lesssim 600\,^{\circ}$C. Thermal modelling, combined with experimentally derived flow laws, suggests that if the Indian lower crust is anhydrous it will remain strong beneath the entire southern half of the Tibetan plateau, as is also suggested by dynamic models. In northwest Tibet, the strong underthrust Indian lower crust abuts the rigid Tarim Basin, and may be responsible for both the clockwise rotation of Tarim relative to stable Eurasia and the gradient of shortening along the Tien Shan.



## 1. Introduction

The distribution of earthquakes provides an important insight into the rheology of continental regions. Rare earthquakes at depths up to ~100 km beneath Tibet have been used to support contrasting views about the vertical distribution of strength within the continental lithosphere (Chen and Molnar, 1983; Chen and Yang, 2004; Monsalve et al., 2006; Priestley et al., 2008). This topic is controversial and important, as it has implications for our understanding of rheology, deformation and topography in continental regions worldwide.

Early views on the connection between seismicity and rheology treated the crust as a homogenous medium, in which the seismic–aseismic transition occurred at 350 °C everywhere (Chen and Molnar, 1983). More recently, the importance of trace amounts of water within crystal lattices has been recognised as affecting the depth of the seismic–aseismic transition in crustal materials. This realisation has led to a revised view of seismicity in the crust, in which the seismic–aseismic transition is thought to be at ~350 °C in hydrous rocks, and up to ~600 °C in anhydrous rocks (Jackson et al., 2008). The proposed ~600 °C temperature limit in anhydrous continental crust is similar to current estimates for the temperature cut-off of earthquakes in the oceanic mantle (McKenzie et al., 2005). However, debate continues about the existence and significance of continental mantle seismicity, and the relation between the seismic–aseismic transition and the distribution of lithospheric strength (Chen and Yang, 2004; Monsalve et al., 2006; Priestley et al., 2008; Burov, 2010).

In slowly deforming areas, the thermal structure is close to steady-state, and easily comparable to the distribution of earthquakes (e.g., Sloan et al., 2011). However, in these relatively undeforming regions it is difficult to probe the rheology of the lithosphere, which requires knowledge of the distribution of strain-rates. We therefore focus on the Tibetan Plateau, which is rapidly deforming, and is far from thermal steady state. The purpose of this paper is to show that the distribution of earthquakes beneath the Tibetan Plateau can be linked, through simple calculations, to the evolution of temperature and rheology within the India–Asia collision zone, and hence integrated into our understanding of continental rheology and dynamics.

We first present new results for earthquake depths across the Tibetan plateau. We then describe the results of thermal models that can provide insights into this observed earthquake distribution, and how it relates to the rheological structure of the India–Asia collision zone. Finally, we discuss the implications of our results for the tectonics of Central Asia, north of the Tibetan Plateau.

## 2. Earthquake locations

By using array-stacking techniques and coherency analyses (Heyburn and Bowers, 2008) for small-aperture seismic arrays at teleseismic distances (30–90°), we have observed and identified the direct arrival (*P*) and subsequent depth phases (*pP*, *sP*) for

* Corresponding author.
*E-mail addresses:* tjc52@esc.cam.ac.uk, tjc52@cam.ac.uk (T.J. Craig).

0012-821X/$ - see front matter © 2012 Elsevier B.V. All rights reserved.
http://dx.doi.org/10.1016/j.epsl.2012.07.010

smaller earthquakes in the region of the Tibetan Plateau than have previously been analysed using teleseismic data.

For seven arrays in North America, Europe and Australia, the expected back-azimuth and slowness for a given event were calculated based on the best available earthquake location (from the EHB catalogue if available (Engdahl et al., 1998), or the NEIC if not), with the expected slowness calculated using the ak135 earth model (Kennett et al., 1995). Data from each station within an

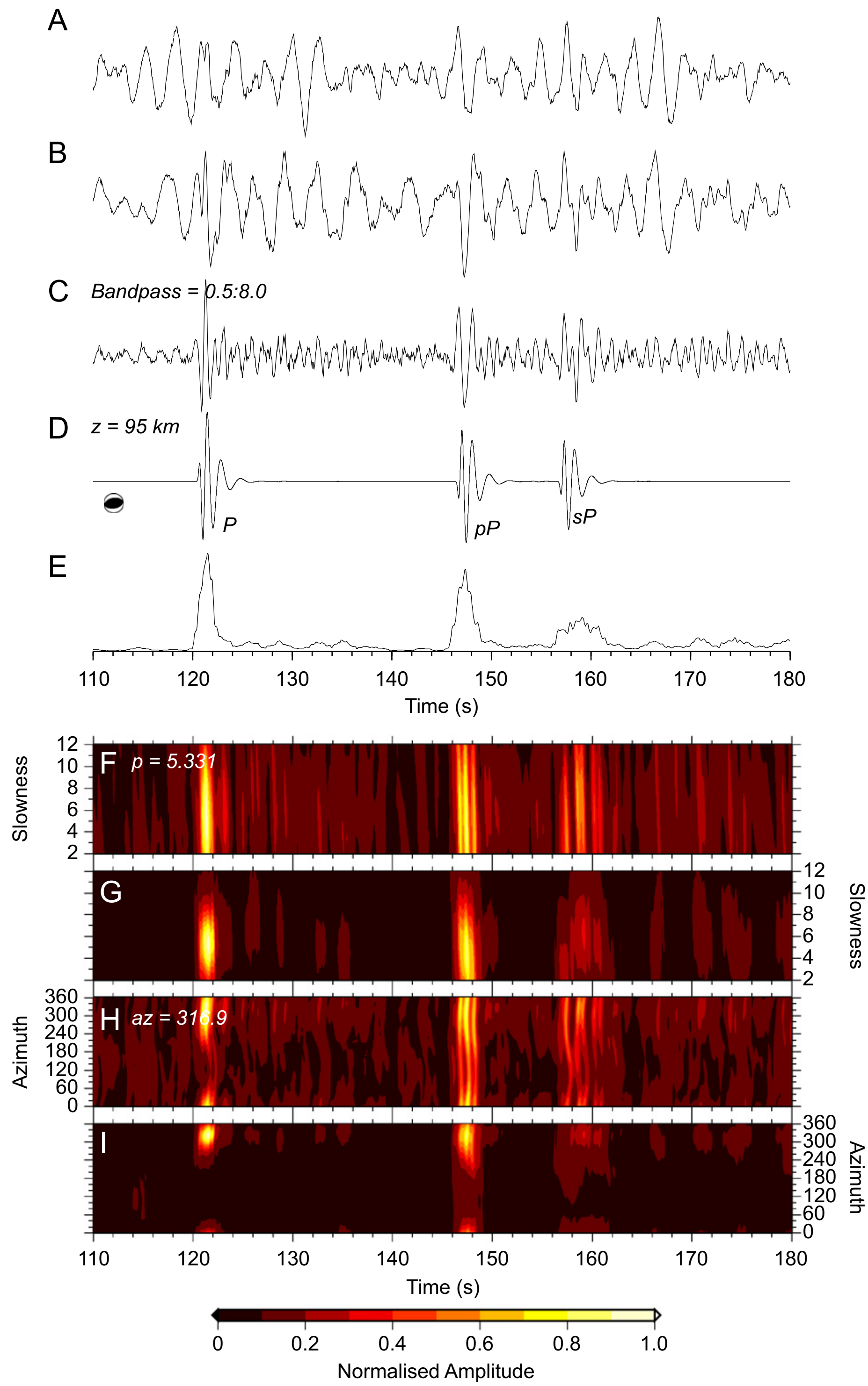


**Fig. 1.** Depth determination using teleseismic arrays. An example of the array processing techniques used in this study for a $M_W$ 4.7 earthquake on 2 April 2011 in northwestern Tibet, recorded at the Alice Springs Array in Australia. (a) Example of an unfiltered seismogram from a single station within the array. (b) Unfiltered beamformed linear stack of all seismograms from the array. (c) Bandpass filtered beamformed linear stack of all seismograms from the array. (d) Synthetic waveform calculated with a depth of 95 km, and the given mechanism. The three principle phases (direct *P*, and the two depth phases *pP* and *sP*) are labelled. (e) *F*-statistic (see text and Heyburn and Bowers, 2008). (f) Beam power as a function of time and slowness (earthquake expected at 5.331 s/°, based on NEIC location). (g) *F*-statistic as a function of time and slowness. (h) Beam power as a function of time and azimuth (earthquake expected at 316.9°, based on NEIC location). (i) *F*-statistic as a function of time and azimuth. The colour scales for (f)–(i) are all normalised to the maximum value within the window shown.

array were then timeshifted, based on the assumption that the wavefront travels as a plane-wave across the array at a uniform velocity (slowness) and from a single direction (back-azimuth), and linearly stacked. Data were also bandpassed in an attempt to isolate the signal of the earthquake and remove unrelated noise. To assist in the correct identification of seismic phases, we used the coherency analyses of Heyburn and Bowers (2008), calculating the *F*-statistic (defined as the power of the beam divided by the average of the power of the difference between the beam and the single-station seismograms from within the array). An example, for a $M_W$4.7 earthquake beneath northwestern Tibet, is shown in Fig. 1.

To confirm that the identified arrivals are from a seismic event at the expected point of origin, we performed a sweep through azimuth and slowness ranges, and discarded phases where the peak in both radiated energy and in coherence occurred at a significantly different origin point from that expected based on the catalogue location. Given the small array aperture required to resolve the relatively high frequency content of such small earthquakes, the spatial resolution is typically quite poor, particularly in slowness (see Fig. 1f–i). Whilst consideration of the signal coherence improves on the resolution of the simple linear stack (Fig. 1g,i), discrimination between origin points separated by $<15^\circ$ or $<1.5-2\ ^\circ/s$ is rarely possible. However, we were able to confirm that the signals we analysed were generated by the events we have selected in the region of the Tibetan Plateau, and were not from events elsewhere in the world at similar times.

Once multiple depth phases had been identified, forward modeling of the waveforms was then used to constrain the focal depths. We used velocity structures based on the *S*-wave velocity models of Acton et al. (2010) for the India–Asia region, with *P*-wavespeeds calculated using $V_p/V_s$ ratios based on those determined by Monsalve et al. (2008) for a transect across the Himalayas from peninsular India into Tibet. Outside the Tibetan Plateau, we used $V_p/V_s=1.74$. Within the Plateau, we use $V_p/V_s=1.65$ at $<40$ km depth, and $V_p/V_s=1.74$ at $>40$ km depth. Synthetic seismograms were calculated using the WKBJ algorithm (Chapman et al., 1988), assuming the CMT mechanism if available, or one consistent with the relative amplitudes of the observed phases. This technique yielded a total of 69 new earthquake depths (Table S1). Uncertainties arose principally from the accuracy in phase identification, and the accuracy of the velocity model. For phase identification, which is non-systematic, we estimate this uncertainty to be $\pm 3$ km, based on the ability to pick phase arrivals to within half the typical duration of the pulse width. Errors from the velocity model will be systematic to the dataset, and depth dependent. Based on a 10% perturbation in the velocities used, we estimate these to range from $\pm 1$ km at shallow depths, to $\pm 9$ km at $\approx 100$ km, leading to an overall error estimate between $\pm 4$ km at shallow depth and $\pm 12$ km at around 100 km.

In addition, 25 other new larger-magnitude earthquakes ($M_W \geq 5.5$) were modelled using the body-waveform inversion techniques described in detail in Sloan et al. (2011) (Table S2). This method inverts *P* and *SH* waveform shape and amplitude for the depth, mechanism and magnitude of larger earthquakes. Numerous previous studies have also determined accurate earthquake depths within the India–Asia collision zone, which are plotted along with our results in Fig. 2. The studies from which these earthquakes were taken are detailed in the supplementary material. Our new well-located earthquakes provide insights into the seismicity of the Tibetan Plateau. Previously described isolated deep earthquakes (e.g., Chen and Yang, 2004; Priestley et al., 2008) can now be seen to form part of seismogenic layers continuous in the direction of the overall convergence in the deep interior of the range, and the numbers of events observed make the distribution patterns robust.

While earthquakes at shallow ($<20$ km) depths are observed across the whole of Tibet and the surrounding active regions, earthquakes deeper than 40 km are observed only in restricted areas. Earthquakes up to 300 km deep are observed in the Hindu Kush Deep Seismic Zone and the Burmese Arc (enclosed by dashed black lines, Fig. 2a), and occur in recognisable steeply inclined slab-like zones, which are not considered further here. Deep earthquakes outside these areas in Fig. 2a occur only within the Tibetan Plateau, and are restricted to patches in NW Tibet (73–78 °E) and the eastern Himalayas (85–93 °E). A similar picture of the earthquake depth distribution for restricted areas emerges from sparse local seismic surveys (e.g., Langin et al., 2003; Monsalve et al., 2006; Liang et al., 2008).

Significant effort was put into investigating possible deep earthquakes between the two observed patches, beneath south-central Tibet (region A in Fig. 2a). Routine catalogues (e.g., NEIC, EHB) report earthquakes in this region at depths exceeding the 20 km typically seen in Tibet, but lack the accuracy in depth required for our purposes. However, despite analysing all reported earthquakes at depths $>20$ km, with $M_W>4.5$, since 2005, all events in this region either occurred at shallow depth, or failed to yield a depth that was robust and reliable. We are therefore unable to confirm the presence of any deep seismicity in this region.

Fig. 2d shows earthquake depths within India and the Tibetan Plateau as a function of distance from the Himalayan front (solid black line, Fig 2a.), projected along the India–Asia convergence vector. Although care must be taken when interpreting events significantly off the line of projection, some clear patterns emerge. Peninsular India has earthquakes throughout the thickness of the crust, as is most visible around the Shillong Plateau and the 2001 Bhuj earthquake (*S* and *B* in Fig. 2a), and a small number of earthquakes extend to depths of $48\pm5$ km, potentially into the top of the upper mantle. Beneath the Himalayas, earthquakes also occur throughout the crust and possibly into the uppermost 10–15 km of the mantle (Monsalve et al., 2006). Beneath Tibet, beyond $\sim 200$ km north of the Himalayan front, the earthquake distribution is more complex. Shallow earthquakes occur across the whole plateau at depths $<20$ km, and beneath this the mid-crust is generally aseismic (with the exception of two small events labeled *K* in Fig. 2d, in northwest Tibet, discussed later). Beneath Tibet, deep earthquakes are also present in a 10–30 km thick band close to the Moho, but only in the two patches described above, which are within $\sim 500$ km of the Himalayan front.

## 3. Temperature structure

We now consider how the thermal structure in the region relates to the earthquake distribution. Evidence from surface-wave tomography and from mantle xenoliths indicates that the lithosphere under peninsular India is $\sim 150-200$ km thick, and that the uppermost $\sim 10$ km of the mantle is likely to be colder than 600 °C (Priestley et al., 2008). The distribution of earthquakes in India is therefore easily explained, provided the lower crust is largely anhydrous and thereby capable of producing earthquakes at temperatures up to approximately 600 °C (Mackwell, 1998; Jackson et al., 2008).

Previous thermal models for the India–Asia collision have predominantly focused on the fine-scale thermal structure of the Himalayas, to analyse thermochronological and thermobarometric data (e.g., Bollinger et al., 2006; Herman et al., 2010). However, these models have not focused on the deeper thermal structure in the lower crust and uppermost mantle beneath Tibet, as is required to investigate the relationship between temperature and the deep earthquakes beneath the plateau. Although Priestley et al. (2008) conducted a one-dimensional diffusion calculation for the Indian

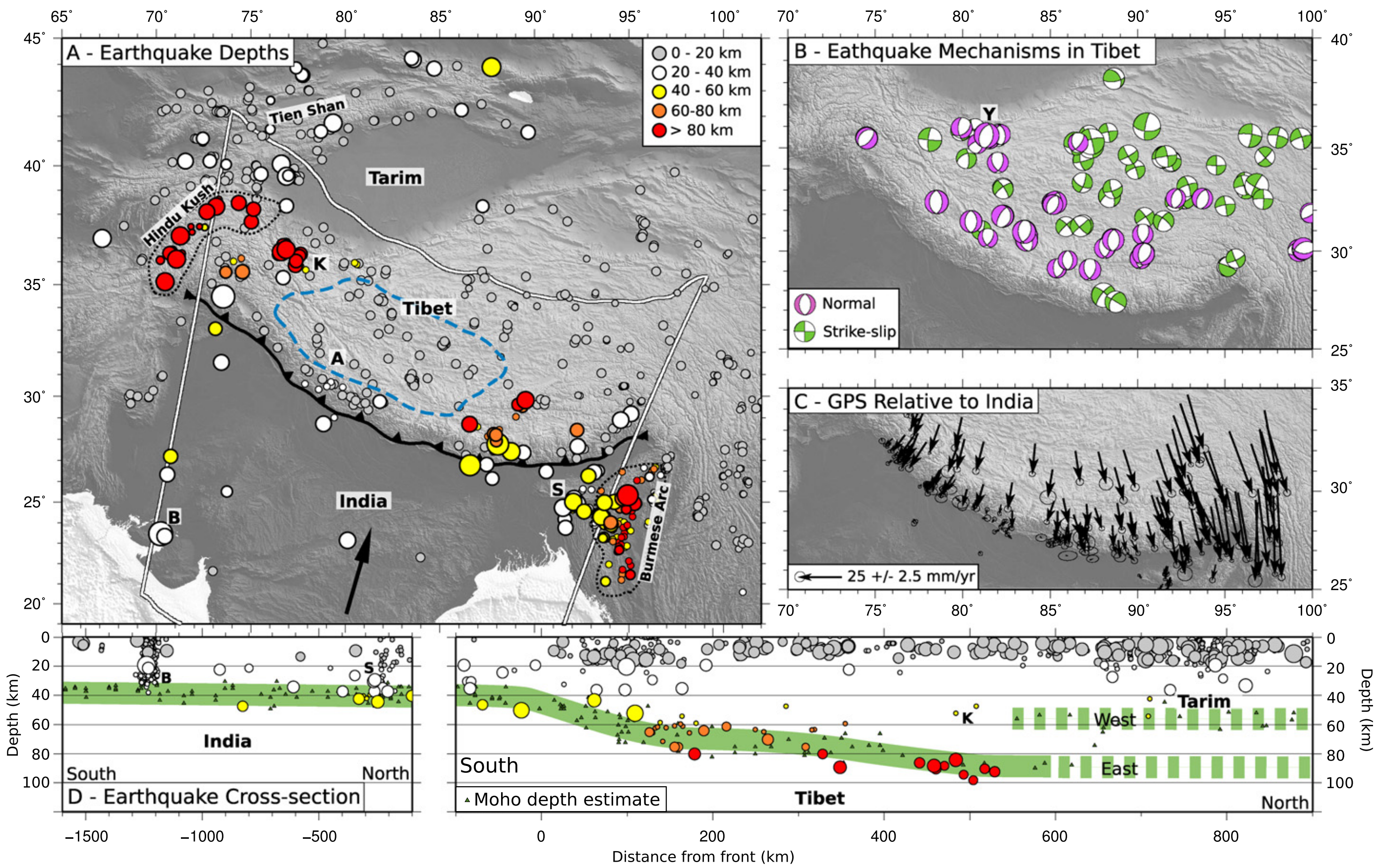


**Fig. 2.** Seismicity and deformation across the India–Asia collision. (a) Map of earthquakes with accurately constrained depths, from this study (Tables S1 and S2) and others (see supplementary material). Depths are indicated by colour, and earthquakes deeper than 20 km are scaled by magnitude. Black arrow indicates the India–Asia convergence vector. The dashed blue line (*A*) outlines the area in central southern Tibet where there is no deep seismicity. *B*: 2001 Bhuj earthquake. *S*: Shillong Plateau. *K*: mid-crustal earthquakes beneath NW Tibet (Huang et al., 2011). (b) Normal (purple) and strike-slip (green) focal mechanisms across the Tibetan Plateau from the GCMT catalogue (depth $\leq 40$ km, $M_W \geq 5.5$, only well constrained mechanisms with a % double couple $\geq 70\%$). *Y* indicates the 2008 Yutian earthquake. (c) GPS velocities in southern Tibet, relative to India (Banerjee et al., 2008). (d) Earthquake cross section, with earthquakes within the white box in (a) reprojected as a function of distance from the Himalayan front, along the India–Asia convergence vector. Earthquakes in the Hindu Kush Deep Seismic Zone and the Burmese Arc (dashed black lines in (a)) are excluded. The green band encompasses published receiver function estimates for the Moho from within the white box in (a) (green triangles; see supplementary material). (For interpretation of the references to color in this figure caption, the reader is referred to the web version of this article.)

plate, the importance of thermal advection in Tibet requires a more complex model. We have therefore constructed our own thermal model to investigate how the temperature structure relates to the pattern of earthquakes beneath Tibet.

We model the plateau in two dimensions using the finite-difference method, taking into account horizontal and vertical diffusion of heat, the horizontal and vertical advection of material associated with the relative motion between India and Tibet, and radiogenic heat production. Conductivities, heat capacities and densities are determined as a function of temperature using the expressions given in McKenzie et al. (2005) and Nabelek et al. (2010). Several parameters in such thermal models are poorly constrained, particularly the rates of radiogenic heating at depth and the model kinematics. However, by making reasonable assumptions based on available observations and insights from previous models (e.g. Henry et al., 1997; Bollinger et al., 2006; Herman et al., 2010), we can estimate the major characteristics of the thermal structure beneath Tibet (Figs. 3 and S1).

The geometry and kinematics of our model are summarised in Fig. 3a. India, in initial thermal steady state, starts horizontal across the model. The orogenic front marking the leading edge of Tibetan crust starts at the north end of the model, and moves gradually southwards through time, overriding the Indian crust and mantle. The overthrusting material has a thickness of 45 km, which tapers over a distance of 200 km to zero at the leading edge. The frame of reference is fixed to India. Models are run for 50 Myrs (the approximate age of the collision). Velocities in our model are constant through time, and imposed based on values consistent with high-end estimates for late Cenozoic deformation (convergence at 22 mm yr$^{-1}$, with 4 mm yr$^{-1}$ of overthrusting; Henry et al., 1997; Lavé and Avouac, 2000).

We model a scenario in which India is underthrust beneath Tibet in a ramp-and-flat geometry, reflecting a combination of the southwards-relative flow of Tibetan material over India, and the northwards-relative underthrusting of India. Previous studies have focused on the effect of accretion of Indian material onto the southern edge of Tibet by transmission across the plate interface, determining relatively low accretion rates ($\sim 60$ km$^2$ Myr$^{-1}$; Bollinger et al., 2006). We have therefore included in our model 5 km of accretion from the top of the Indian crust into the Himalayas as our preferred model (Fig. 3a). Changing the degree of accretion to be zero or double the amount shown in Fig. 3 has little effect on the part of our model where the deep earthquakes are detected. Tests to demonstrate the effects of varying the accretion are shown in Fig. S2.

For India, we use an initial steady-state geotherm, based on a crustal thickness of 40 km (see Fig. 2d) and a lithospheric thickness of 175 km, constrained by xenolith data from southern India and surface-wave derived estimates of temperatures (Priestley et al., 2008). The surface is maintained at 0 °C, and the base of the lithosphere is maintained at a mantle potential temperature of

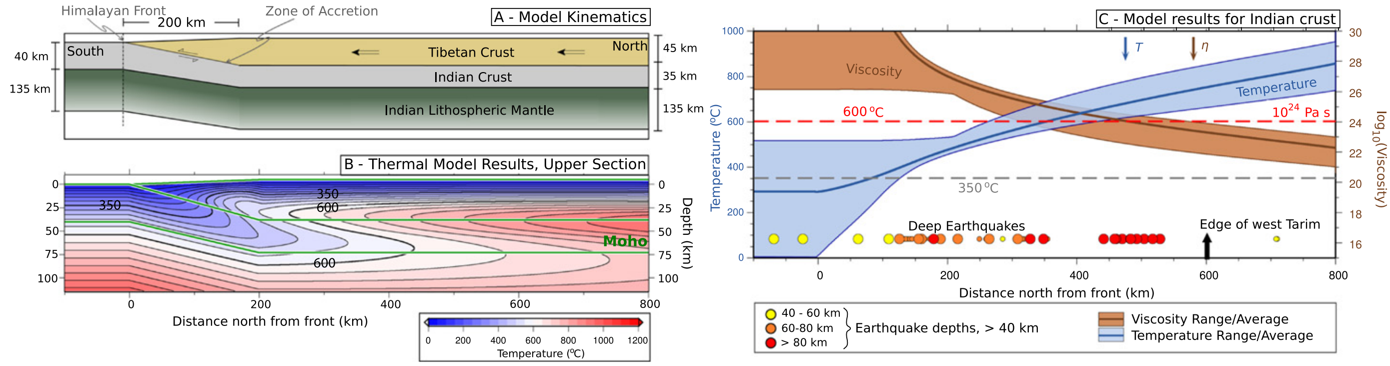


**Fig. 3.** Thermal modeling of India underthrusting Tibet. (a) Structure of the two-dimensional thermal model. (b) Calculated temperatures for the top section of our preferred model, presented in full in supplementary material. Contours are at 50 °C intervals. Green lines represent boundaries between Tibetan crust, Indian crust, and mantle. (c) Temperature (blue) and viscosity (brown) estimates for the Indian crust (grey region, (a)). For both temperature and viscosity, the thick dark line indicates the average, with the lighter shaded area indicating the range. Viscosities are calculated using a dry anorthite flow-law (Rybacki and Dresen, 2000) at a strain rate of $3\times10^{-9}\,\mathrm{yr}^{-1}$ and using a grain size of 1 mm. Deep earthquakes are shown as a function of distance from the front, coloured as in Fig. 2. The blue arrow indicates the distance at which temperatures fall below those expected to cut of seismicity. The brown arrow indicates the distance at which viscosities fall below the criterion required to explain surface extension. The southern extent of the topographic low of the Tarim basin is indicated by the black arrow. (For interpretation of the references to color in this figure caption, the reader is referred to the web version of this article.)

1315 °C. Observed surface heat-flow measurements across northern India have average values in the range 45–70 $\mathrm{mW\,m^{-2}}$ (after Roy and Rao, 2000), which constrains the total crustal heat production and mantle heat flux. The input model used here has a surface heat flux of 61 $\mathrm{mW\,m^{-2}}$. For radiogenic heating, we use two crustal layers in India, with values of 2.0 $\mu\mathrm{W\,m^{-3}}$ (upper crust) and 0.4 $\mu\mathrm{W\,m^{-3}}$ (lower crust), consistent with a slightly enriched gneissic upper crust (Roy and Rao, 2003) overlying a depleted granulitic lower crust (Jaupart and Mareschal, 1999; Roy and Rao, 2003), with an interface at 20 km.

The upper (Tibetan) crustal material input into the model at the northern edge has the northern Tibet geotherm derived from crustal xenoliths (Hacker et al., 2000). For Tibetan material, we do not have accurate constraints on the distribution of radiogenic heat production with depth. Surface measurements of heat production from the Himalayas are usually high ($>1\,\mu\mathrm{W\,m^{-3}}$), but the source of such values is complicated by the inclusion of Indian derived material into the wedge. The origin of material sourced from the northern side of the collision is complex, comprising a series of accreted terranes and island arcs, and the distribution of radiogenic heat production is unlikely to be as uniform as in ancient continental crust. Given the lack of precise constraint, we assume a single average value for all Tibetan material, in this case taken to be 1.5 $\mu\mathrm{W\,m^{-3}}$. Tests varying this value indicate that it predominantly affects the temperature evolution in Tibetan material and at the top of the underthrust Indian crust, and hence the initial point of inversion in the vertical temperature gradients (Fig. 3b), whilst its influence on the temperatures near the Indian Moho, which is the focus of this study, is minor when compared to other factors.

In our model (Figs. 3b,c and S1), as India is underthrust beneath southern Tibet, it heats up because of the emplacement of hot and radiogenic heat-producing Tibetan crust above it. The Indian lower crust heats up slowly during underthrusting, and the calculations show that by ~20 Myrs it is the coolest part of the Indian crust, indicating why the lower crust remains seismic, whilst the mid-crust above it is aseismic within Tibet. Our models show that the 600 °C isotherm in the Indian lower crust can extend horizontally for ~450–500 km beneath the Tibetan Plateau. Changing the model parameters, particularly advective velocities, within reasonable ranges can move the extent of the 600 °C isotherm by up to ~150 km, but the essential shape of the isotherms remains similar. Variations in accretion rates and the radiogenic heating in Tibet influence the distance to the initial point of inversion of the vertical thermal gradient, but have a lesser effect on the on the deeper structure within the plate (see Fig. S2). The model shown in Figs. 3 and S1 demonstrates that, with reasonable assumptions for poorly constrained parameters, the observed seismicity is consistent with an understanding of continental rheology in which seismicity can persist to ~600 °C in anhydrous lower crust or in mantle material (Jackson et al., 2008). Deep earthquakes beneath Tibet are thus reasonably explained by the cold Indian lowermost crust and uppermost mantle, displaced downwards by underthrusting beneath Tibet, heating up slowly enough to remain seismogenic long after the overlying material has been heated beyond the seismic–aseismic transition.

## 4. Relationship to surface tectonics

The style of active tectonics at the surface of Tibet is likely to be governed by the rheology of India at depth (Copley et al., 2011). Earthquake focal mechanisms at shallow depth within the plateau (Fig. 2b) show a clear division between southern Tibet, where the dominant faulting is east-west extension on north-south striking normal faults, and northern Tibet, where conjugate strike-slip faulting accommodates north-south shortening and east-west extension. There are some exceptions to this pattern, but these are likely to be the result of local kinematic effects, such as the Yutian normal fault system, labelled *Y* in Fig. 2b, which is linked to the change in strike of the Altyn–Tagh strike-slip fault (Furuya and Yasuda, 2011). The same pattern can be seen in GPS data (Fig. 2c; Gan et al., 2007; Banerjee et al., 2008), which is interpreted in southern Tibet to show east-west extension and transient elastic strain accumulation around the Himalayan thrust faults, and in northern Tibet to show permanent north-south shortening and east-west extension. The transition between the two tectonic regimes occurs 600 ± 100 km north of the Himalayan front, slightly beyond the northernmost deep earthquakes.

Dynamic models suggest that the presence of pure east-west extension in southern Tibet indicates that the surface is mechanically coupled to the underthrust Indian lithosphere, which must have a high enough viscosity ($\geq 5\times10^{23}$ Pa s) to act as a rigid base to the flow of the overlying crust (Copley et al., 2011). Using our thermal model and experimentally derived mineral flow-laws, we can estimate the viscosity of the Indian crust beneath

Tibet. Fig. 3c shows estimated viscosities in the underthrust Indian lower crust, calculated using a dry anorthite flow-law (Rybacki and Dresen, 2000), a grainsize of 1 mm, and a strain-rate of $3 \times 10^{-9}\ \mathrm{yr}^{-1}$ (an order of magnitude less than the observed strain-rate at the surface). With this dry anorthite flow-law, our calculated viscosities fall below $5 \times 10^{23}$ Pa s slightly ($\sim$100 km) north of the limit of deep earthquakes, in agreement with the transition between tectonic regimes at the surface (Fig. 3c). Other flow-laws would obviously produce different results. However, we can conclude that our thermal model is consistent with the observed tectonics of Tibet if the Indian lower crust is anhydrous and contains significant plagioclase, in line with previous suggestions of an anhydrous granulite rheology (Cattin et al., 2001; Priestley et al., 2008), and with our conclusions regarding the thermal control on the deep seismicity.

Our proposed rheological model, in which a rigid, strong India persists to significant distances beneath the plateau, is consistent with measured seismic anistropy beneath Tibet. The significant anisotropy observed in north and northeastern Tibet contrasts with the isotropic or weakly anisotropic fabric of peninsular India and southern and western Tibet (Zhao et al., 2010). This transition may reflect where the underlying Indian material becomes hot and weak enough to deform significantly, and develop an anisotropic fabric.

## 5. Central southern Tibet

A striking feature of Fig. 2a is the lack of earthquakes deeper than 20 km beneath central-southern Tibet (region A). Both surface- and body-wave tomography indicate that all of southern Tibet is underlain by high velocity Indian material, with no resolvable along-strike variation (Priestley et al., 2008; Li et al., 2008; Hung et al., 2011). One possible explanation for the lack of deep earthquakes might be that the Indian crust in this region is too hot to deform in earthquakes (for example, due to higher radiogenic heating). However, allowing the parameters in our thermal models to vary within reasonable ranges only moves the isotherms (and hence the expected extent of seismicity) southwards, and cannot heat the entire Indian lower crust in this region to temperatures above 600 °C. Similarly, influences on the thermal structure from deeper in the mantle would again simply push the cutoff of seismicity southwards, and would not be expected to heat the entire region above the seismogenic limit.

Alternatively, the absence of deep seismicity in region A might be related to a lower crust of different composition (e.g. more hydrated or quartz-rich), deforming by ductile flow rather than failure in earthquakes. However, we can use numerical experiments to suggest that a lateral variation in mineral composition, and hence strength, would be mirrored by a change in the surface tectonics.

Fig. 4a shows the results of a calculation by Copley et al. (2011), who constructed a model of the deformation of a plateau subjected to compression between bounding plates and gravity-driven flow. They suggested that for pure east-west extension to occur in southern Tibet, rigid Indian lower crust must underlie the entire southern half of the plateau. To directly investigate if an along-strike variation in lower crustal rheology would be revealed in the surface tectonics, we have performed additional calculations to test if the aseismic region in central southern Tibet could have a

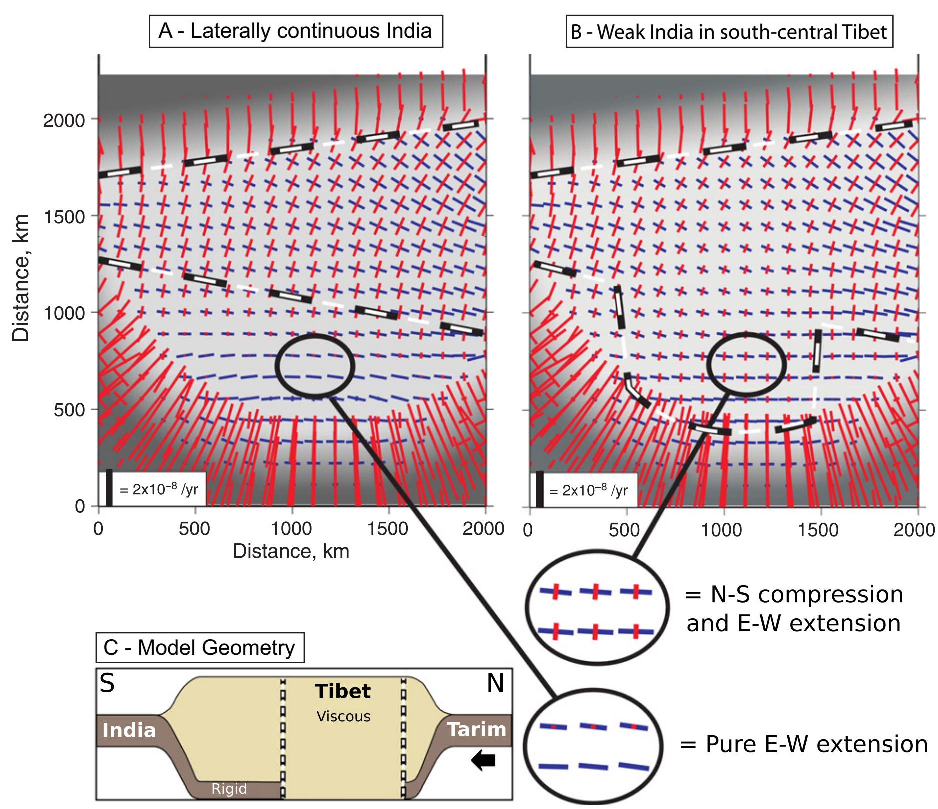


**Fig. 4.** Dynamic models relating surface deformation to lower crustal rheology. (a) The calculation shown in Copley et al. (2011), in which rigid lower crust underlies the entire southern half of the plateau (south of the southernmost dashed line; see (c) for model geometry). The coloured bars represent the principal axes of the horizontal strain-rate tensor, with isolated blue bars representing horizontal extension, isolated red bars representing horizontal compression, and coupled red and blue crosses being equivalent to strike-slip deformation. Note the pure east-west extension in the southern plateau (inset). (b) Calculation identical to (a), except that the part of the lower crust corresponding to region A in Fig. 2a has been weakened relative to the other underthrust material. Again, the lower crust is only rigid south of the southernmost dashed line. Note the combination of east-west extension and north-south shortening in the southern plateau (inset). (c) Cartoon of the model geometry. Dark regions are rigid, with imposed velocities. The lighter region deforms by viscous flow in response to the applied India–Tarim convergence, and gravitational potential energy contrasts. (For interpretation of the references to color in this figure caption, the reader is referred to the web version of this article.)

different rheology to the seismogenic material to the east and west, and yet still produce a pattern of surface deformation consistent with the observations. The results of such a calculation are shown in Fig. 4b, in which the lower crust in the part of the model corresponding to region A has been weakened relative to the rest of the underthrusting lower crust. In this situation, the predicted surface tectonics in the southern part of the model plateau is a mix of east-west extension and north-south compression, at odds with the observed faulting in southern Tibet (Fig. 2b,c and Section 4). Given the dominance of normal faulting across southern Tibet, it therefore appears that the aseismic region A is not likely to be significantly weaker than the seismically active parts of underthrusting India to the east and west.

We therefore conclude that the reason for the rarity of deep earthquakes, and for their absence in south-central Tibet during our observation period, is likely to be that the Indian lower crust is too strong to break in response to the forces being exerted on it, or that the strain rates are so low that earthquake repeat times are extremely long. In this context, it is regions where earthquakes have been observed that may be anomalous, possibly due to a spatially limited influx of fluids (Lund et al., 2004), or local structural heterogeneities or triggering (analogous, perhaps, to the uneven concentrations of events within peninsular India around the Shillong Plateau and in the vicinity of the Bhuj earthquake).

## 6. Implications for regional tectonics

Our results have implications for the kinematics of deformation in central Asia. In northwest Tibet, seismogenic Indian lithosphere underthrusts far enough north to be in contact with the lithosphere of the western Tarim Basin, which is in turn underthrust beneath the northern edge of Tibet, and whose limit is observed as a sharp step in the Moho (Fig. 2d; Wittlinger et al., 2004). Collision between the rigid Indian and Tarim lithospheres at depth beneath the northwestern Tibetan Plateau will impart a northwards push to the western end of the Tarim Basin. In doing so, it will provide a force to drive the observed clockwise rotation of the Tarim Basin relative to stable Eurasia and the westwards-increasing convergence taken up across the Tien Shan (Chen et al., 1991; Avouac et al., 1993; Zubovich et al., 2010). The unusually large number of earthquakes at 80–100 km beneath NW Tibet, accompanied by some minor earthquakes at mid-crustal levels (Huang et al., 2011; labelled *K* in Fig. 2a,d), may then be explained by stress concentrations and high strain-rates near the India–Tarim contact, combined with the cooling effect on the overlying crust resulting from the proximity of both cold Tarim and cold Indian lithospheres.

The timing of events within the India–Asia collision remains, to some extent, controversial. However, simple calculations based on the rates of plate convergence between India and Asia (Copley et al., 2010), paleomagnetic estimates for the shortening accommodated within the Tibetan Plateau itself (Tan et al., 2010; Sun et al., 2012), and the present-day separation of the Tarim basin from the Himalayan Front, indicate that the collision at depth between the Indian and Tarim lithospheres is expected to have occurred sometime in the range 20–40 Ma (see Fig. S3). Notably, this timing coincides with the initiation of compression north of the Tarim basin in the Tien Shan (30–25 Ma; Glorie et al., 2011) and the Altai (25–20 Ma; Yuan et al., 2006), and the start of significant sedimentation in the Tarim and Junggar basins (Miocene onwards; Métivier and Gaudemer, 1997). We are not able to state definitively if this agreement in timing is causative rather than coincidence, but we can conclude that the dates of initiation of mountain building in central Asia are consistent with our suggestions regarding the forces exerted upon Tarim by India.

The present-day convergence between western India and Asia is accommodated by a combination of shortening between India and Tarim, and convergence distributed across the Tien Shan and further north. The different surface velocities measured by GPS in India and Tarim indicate that the two cannot be completely mechanically coupled where they meet at depth beneath NW Tibet. However, it is likely that the high strain-rates associated with their contact will permit the transmission of large compressive stresses between them. Some of the convergence between India and Tarim is likely to be occurring by the loss of material from the leading end of India, as it heats up and is expelled out of the collision between the two otherwise rigid bodies.

## 7. Conclusion

In conclusion, our view of the seismicity, rheology and tectonics of Tibet is summarised in Fig. 5. The underthrusting beneath Tibet

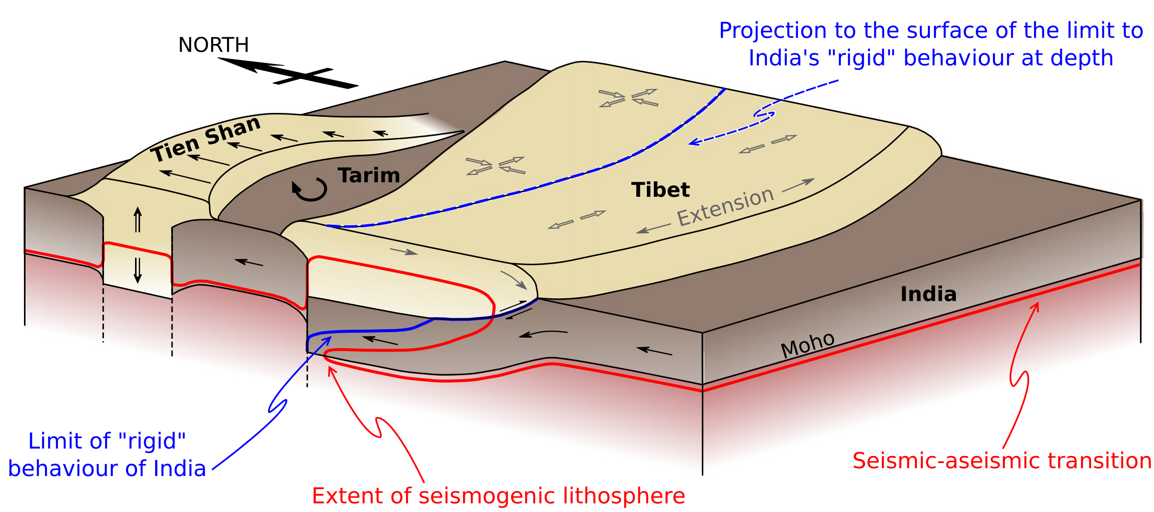


**Fig. 5.** Schematic sketch of the tectonics and structure of the India–Asia collision zone. Black arrows indicate velocities with respect to stable Eurasia. Grey arrows represent velocities with respect to peninsular India. Grey double arrows within Tibet are indicative of the local strain field. The red line indicates the seismic-aseismic transition. Blue lines indicate the extent of the rigid behaviour of India at depth (solid) and its projection to the surface (dashed). Rotation of the Tarim basin relative to Eurasia, and westwards increasing compression across the Tien Shan, may be driven by the collision between the rigid extent of India and the Tarim basin at depth beneath northwest Tibet. (For interpretation of the references to color in this figure caption, the reader is referred to the web version of this article.)

of cold, rigid and seismogenic Indian lower crust, which heats up slowly as it is overridden by hot Tibetan material, results in seismicity extending beneath the plateau at the base of the Indian crust and possibly the top of the Indian mantle. This cold Indian material retains a sufficiently high viscosity to act as a rigid base to the flowing Tibetan crust, resulting in east-west extension at the surface in southern Tibet. The collision beneath northwestern Tibet of rigid Indian lower crust with Tarim may drive the rotation of Tarim with respect to Asia, and contribute to the westwards-increasing shortening taken up by the Tien Shan.

## Acknowledgments

We thank two anonymous reviewers, and the Editor for comments that improved the manuscript. We also thank D. McKenzie and K. Priestley for useful discussions, and R. Heyburn for use of his array processing code. Seismograms were retrieved from the IRIS DMC, and from the Seismological Central Observatory (SZGRF). T.J.C. is supported by a Girdler scholarship from the University of Cambridge. A.C. is supported by a research fellowship at Pembroke College in the University of Cambridge. All authors also thank a NERC-NCEO Grant to COMET+ for additional support.

## Appendix A. Supplementary data

Supplementary data associated with this article can be found in the online version at http://dx.doi.org.10.1016/j.epsl.2012.07.010.

## References

Acton, C.E., Priestley, K., Gaur, V.K., Rai, S.S., 2010. Group velocity tomography of the Indo-Eurasian collision zone. J. Geophys. Res. 115 , http://dx.doi.org/10.1029/2009JB007021.

Avouac, J.-P., Tapponnier, P., Bai, M., You, H., Wang, G., 1993. Active thrusting and folding along the northern Tien Shan and late cenozoic rotation of the Tarim relative to Dzungaria and Kazakhstan. J. Geophys. Res. 98, 6755–6804.

Banerjee, P., Bürgmann, R., Nagarajan, B., Apel, E., 2008. Intraplate deformation of the Indian subcontinent. Geophys. Res. Lett. 35 , http://dx.doi.org/10.1029/2008GL035468.

Bollinger, L., Henry, P., Avouac, J.-P., 2006. Mountain building in the Nepal Himalaya: thermal and kinematic model. Earth Planet. Sci. Lett. 244, 58.

Burov, E., 2010. The equivalent elastic thickness ($T_e$), seismicity and the long-term rheology of continental lithosphere: time to burn-out 'crème brûlée'? Insights from large-scale geodynamic modeling. Tectonophysics 484, 4–26.

Cattin, R., Martelet, G., Henry, P., Avouac, J.P., Diament, M., Shakya, T.R., 2001. Gravity anomalies, crustal structure and thermo-mechanical support of the Himalaya of Central Nepal. Geophys. J. Int. 147, 381–392.

Chapman, C., Yen-Li, C., Lyness, D., 1988. The WKBJ seismogram algorithm. In: Doornbos, D. (Ed.), Seismological Algorithms: Computational Methods and Computer Programs. Academic Press Limited, London, I.2,47–74.

Chen, W.-P., Molnar, P., 1983. Focal depths of intracontinental and intraplate earthquakes and their implications for the thermal and mechanical properties of the lithosphere. J. Geophys. Res. 88, 4183–4214.

Chen, W.-P., Yang, Z., 2004. Earthquakes beneath the Himalayas and Tibet: evidence for strong lithospheric mantle. Science 304 , http://dx.doi.org/10.1126/science.1097324.

Chen, Y., Cogne, J.-P., Courtillot, V., Avouac, J.-P., Tapponier, P., Wang, G., Bai, M., You, H., Li, M., Wei, C., Buffetaut, E., 1991. Paleomagnetic study of mesozoic continental sediments along the Northern Tien Shan (china) and heterogenous strain in Central Asia. J. Geophys. Res. 96, 4065–4082.

Copley, A., Avouac, J.-P., Royer, J.-Y., 2010. India–Asia collision and the Cenozoic slowdown of the Indian plate: implications for the forces driving plate motions. J. Geophys. Res. 115 , http://dx.doi.org/10.1029/2009JB006634.

Copley, A., Avouac, J.-P., Wernicke, B.P., 2011. Evidence for mechanical coupling and strong Indian lower crust beneath southern Tibet. Nature 472, 79–81 , http://dx.doi.org/10.1038/nature09926.

Engdahl, E.R., van der Hilst, R.D., Buland, R.P., 1998. Global teleseismic earthquake relocation with improved travel times and procedures for depth determination. Bull. Seismolog. Soc. Am. 88, 722–743.

Furuya, M., Yasuda, T., 2011. The 2008 Yutian normal faulting earthquake ($M_W$), NW Tibet: non-planar fault modeling and implications for the Karakax Fault. Tectonophysics 511, 125–133, http://dx.doi.org/10.1016/j.tecto.2011.09.003.

Gan, W., Zhang, P., Shen, Z.-K., Niu, Z., Wang, M., Wan, Y., Zhou, D., Cheng, J., 2007. Present-day crustal motion within the Tibetan Plateau inferred from GPS measurements. J. Geophys. Res. 112 , http://dx.doi.org/10.1029/2005JB004120.

Glorie, S., Grave, J.De., Buslov, M.M., Zhimulev, F.I., Stockli, D.F., Batalev, V.Y., Izmer, A., Van den haute, P., Vanhaecke, F., Elburg, M.A., 2011. Tectonic history of the Kyrgyz South Tien Shan (Atbashi-Inylchek) suture zone: the role of inherited structures during deformation-propagation. Tectonics 30 , http://dx.doi.org/10.1029/2011TC002949.

Hacker, B.R., Gnos, E., Ratschbacher, L., Grove, M., McWilliams, M., Sobolev, S.V., Wan, J., Zhenhan, W., 2000. Hot and dry deep crustal xenoliths from Tibet. Science 287 , http://dx.doi.org/10.1126/science.287.5462.2463.

Henry, P., Le Pichon, X., Goffé, B., 1997. Kinematic, thermal and petrological model of the Himalayas: constraints related to metamorphism within the underthrust Indian crust and topographic elevation. Tectonophysics 273, 31–56.

Herman, F., Copeland, P., Avouac, J.-P., Bollinger, L., Mahéo, G., Le Fort, P., Rai, S., Foster, D., Pêcher, A., Stüwe, K., Henry, P., 2010. Exhumation, crustal deformation, and thermal structure of the Nepal Himalaya derived from the inversion of thermochronological and thermobarometric data and modeling of the topography. J. Geophys. Res. 115 , http://dx.doi.org/10.1029/2008JB006126.

Heyburn, R., Bowers, D., 2008. Earthquake depth estimation using the *F* trace and associated probability. Bull. Seismolog. Soc. Am. 98, 18–35, http://dx.doi.org/10.1785/0120070008.

Huang, G.-C.D., Roecker, S.W., Levin, V., 2011. Lower-crustal earthquakes in the West Kunlun range. Geophys. Res. Lett. 38 , http://dx.doi.org/10.1029/2010GL045893.

Hung, S.-H., Chen, W.-P., Chiao, L.-Y., 2011. A data-adaptive, multiscale approach of finite-frequency, traveltime tomography with special reference to *P* and *S* wave data from central Tibet. J. Geophys. Res. 116 , http://dx.doi.org/10.1029/2010JB008190.

Jackson, J., McKenzie, D., Priestley, K., Emmerson, B., 2008. New views on the structure and rheology of the lithosphere. J. Geolog. Soc., London 165, 453–465, http://dx.doi.org/10.1144/0016-76492007-109.

Jaupart, C., Mareschal, J.C., 1999. The thermal structure and thickness of continental roots. Lithos 48, 93–114.

Kennett, B.L.N., Engdahl, E.R., Buland, R., 1995. Constraints on seismic velocities in the Earth from travel times. Geophys. J. Int. 122, 108–124.

Langin, W.R., Brown, L.D., Sandvol, E.A., 2003. Seismicity of Central Tibet from Project INDEPTH III seismic recordings. Bull. Seismoglog. Soc. Am. 93, 2146–2159.

Lavé, J., Avouac, J.P., 2000. Active folding of fluvial terrances across the Siwaliks Hills, Himalayas of central Nepal. J. Geophys. Res. 105, 5735–5770.

Li, C., van der Hilst, R.D., Meltzer, A.S., Engdahl, E.R., 2008. Subduction of the Indian lithosphere beneath the Tibetan Plateau and Burma. Earth Planet. Sci. 274, 157–168, http://dx.doi.org/10.1016/j.epsl.2008.07.016.

Liang, X., Zhou, S., Chen, Y.J., Jin, G., Xiao, L., Liu, P., Fu, Y., Tang, Y., Lou, X., Ning, J., 2008. Earthquake distribution in southern Tibet and its tectonic implications. J. Geophys. Res. 113 , http://dx.doi.org/10.1029/2007JB005101.

Lund, M.G., Austrheim, H., Erambert, M., 2004. Earthquakes in the deep continental crust—insights from studies on exhumed high-pressure rocks. Geophys. J. Int. 158, 569–576, http://dx.doi.org/10.1111/j.1365-246X.2004.02368.x.

Mackwell, S.J., 1998. High-temperature deformation of dry diabase with application to tectonics on Venus. J. Geophys. Res. 103, 975–984.

McKenzie, D., Jackson, J., Priestley, K., 2005. Thermal structure of oceanic and continental lithosphere. Earth Planet. Sci. Lett. 233, 337–349, http://dx.doi.org/10.1016/j.epsl.2005.02.005.

Métivier, F., Gaudemer, Y., 1997. Mass transfer between eastern Tien Shan and adjacent basins (central Asia): constraints on regional tectonics and topography. Geophys. J. Int. 128, 1–17, http://dx.doi.org/10.1111/j.1365-246X.1997.tb04068.x.

Monsalve, G., Sheehan, A., Schulte-Pelkum, V., Rajaure, S., Pandey, M.R., Wu, F., 2006. Seismicity and one-dimensional velocity structure of the Himalayan collisions zone: earthquakes in the crust and upper mantle. J. Geophys. Res. 111 , http://dx.doi.org/10.1029/2005JB004062.

Monsalve, G., Sheehan, A., Rowe, C., Rajaure, S., 2008. Seismic structure of the crust and the upper mantle beneath the Himalayas: evidence for eclogitization of lower crustal rocks in the Indian Plate. J. Geophys. Res. 113, http://dx.doi.org/10.1029/2007JB005424.

Nabelek, P.I., Whittington, A.G., Hofmeister, A.M., 2010. Strain heating as a mechanism for partial melting and ultrahigh temperature metamorphism in convergent orogens: implications of temperature dependent thermal diffusivity and rheology. J. Geophys. Res. 115 , http://dx.doi.org/10.1029/2010JB007727.

Priestley, K., Jackson, J., McKenzie, D., 2008. Lithospheric structure and deep earthquakes beneath India, the Himalaya and southern Tibet. Geophys. J. Int. 172, 345–362, http://dx.doi.org/10.1111/j.1365-246X.2007.03636.x.

Roy, S., Rao, R.U.M., 2000. Heat flow in the Indian shield. J. Geophys. Res. 105, 25587–25604.

Roy, S., Rao, R.U.M., 2003. Towards a crustal thermal model for the Archean Dharwar craton, southern India. Phys. Chem. Earth 28, 361–373.

Rybacki, E., Dresen, G., 2000. Dislocation and diffusion creep of synthetic anorthite aggregates. J. Geophys. Res. 105, 26017–26036.

Sloan, R.A., Jackson, J.A., McKenzie, D., Priestley, K., 2011. Earthquake depth distribution in central Asia, and their relations with lithosphere thickness, shortening and extension. Geophys. J. Int. http://dx.doi.org/10.1111/j.1365-246X.2010.04882.x.

Sun, Z., Pei, J., Li, H., Xu, W., Jiang, W., Zhu, Z., Wang, X., Yang, Z., 2012. Palaeomagnetism of late Cretacrous sediments from southern Tibet: evidence for the consistent palaeolatitudes of the southern margin of Eurasia prior to

the collision with India. Gondwana Res. 21, 53–63, http://dx.doi.org/10.1016/j.gr.2011.08.003.
Tan, X., Gilder, S., Kodama, K.P., Jiang, W., Han, Y., Zhang, H., 2010. New paleomagnetic results from the Lhasa block: revised estimation of latitudinal shortening across Tibet and implications for dating the India–Asia collision. Earth Planet. Sci. Lett. 293, 396–404, http://dx.doi.org/10.1016/j.epsl.2010.03.013.
Wittlinger, G., Vergne, J., Tapponnier, P., Farra, V., Poupinet, G., Jiang, M., Su, H., Herquel, G., Paul, A., 2004. Teleseismic imaging of subducting lithosphere and Moho offsets beneath western Tibet. Earth Planet. Sci. Lett. 221, 117–130.
Yuan, W., Carter, A., Dong, J., Bao, Z., An, Y., Guo, Z., 2006. Mesozoic-Tertiary exhumation history of the Altai Mountains, northern Xinjiang, China: new constraints from apatite fission track data. Tectonophysics 412, 183–193, , http://dx.doi.org/10.1016/j.tecto.2005.09.007.
Zhao, J., Yuan, X., Liu, H., Kumar, P., Pei, S., Kind, R., Zhang, Z., Teng, J., Ding, L., Gao, X., Xu, Q., Wang, W., 2010. The boundary between the Indian and Asian tectonic plates below Tibet. Proc. Natl. Acad. Sci. 107, 11229–11233, http://dx.doi.org/10.1073/pnas.1001921107.
Zubovich, A.V., Wang, X.-Q., Scherba, Y.G., Schelochkov, G.G., Reilinger, R., Reigber, C., Mosienko, O.I., Molnar, P., Michajljow, W., Makarov, V.I., Li, J., Kuzikov, S.I., Herring, T.A., W Hamburger, M., Hager, B.H., Dang, Y., Bragin, V.D., Beisenbaev, R.T., 2010. GPS velocity field for the Tien Shan and surrounding regions. Tectonics 29 , http://dx.doi.org/10.1029/2010TC002772.